Electrochemical and PM-IRRAS Studies of the Effect of Cholesterol on the Properties of the Headgroup Region of a DMPC Bilayer Supported at a Au(111) Electrode

Xiaomin Bin[†] and Jacek Lipkowski*

Department of Chemistry, University of Guelph, Guelph, Ontario, Canada N1G 2W1

Received: September 14, 2006; In Final Form: October 20, 2006

Polarization modulation infrared reflection absorption spectroscopy (PM-IRRAS) was employed to investigate the interaction of cholesterol with the headgroups of dimyristoylphosphatidycholine (DMPC) molecules under a static electric field. DMPC/cholesterol (7:3 molar ratio) mixtures form a bilayer on a Au(111) electrode surface by fusion and spreading of small unilamellar vesicles. PM-IRRAS experiments provided detailed information concerning the conformation and hydration of headgroups of DMPC bilayers in the presence and absence of 30% cholesterol. The presence of 30% cholesterol increases the space between the headgroups of DMPC molecules and hence increases the hydration of the DMPC/cholesterol mixed bilayer. The conformational state of the headgroups of DMPC molecules in the mixed bilayer is also significantly changed. The phosphate group is closer to the surface compared with the pure DMPC bilayer. The conformation of the −O−C−C−N moiety changes from gauche to trans in the presence of cholesterol.

Introduction

Cholesterol is a ubiquitous constituent of biological membranes. Incorporation of cholesterol into phospholipid bilayers is known to affect the gel to liquid-crystalline phase transition of model membranes. This effect of cholesterol on lipid bilayers is attributed to its molecular struture. Cholesterol inserts into a membrane bilayer normal to the bilayer plane, with its hydroxyl group in close vicinity to the ester carbonyl of glycerophospholipids, and its alkyl side chain extending toward the bilayer center.[1,2] The hydroxyl group of cholesterol plays an important role in the phospholipid−cholesterol interactions. It has been suggested that it may form a hydrogen bond with either the two C═O groups or the phosphate group of phospholipid molecules,[3−6] but so far there are limited experimental data supporting this suggestion.

In our earlier paper,[7] we described the effect of cholesterol on the properties of the acyl chains of the DMPC bilayer under a static electric field. A membrane with DMPC/cholesterol (7:3) molar ratio was used in this study. That membrane composition gave the lowest capacity and hence ensured the lowest defects density. It was found that the bilayer is detached and separated from the metal surface by a thin cushion of the solvent in the presence of large electric fields and is adsorbed on the metal when the field is small. A dramatic increase of the tilt angle of the acyl chains by 25° to 30° occurs when the bilayer adsorbs at the Au(111) electrode surface. In either the detached or adsorbed state, the tilt angle of the acyl chains with respect to the surface normal is smaller in the presence of cholesterol than that in a pure DMPC bilayer. The addition of cholesterol also leads to an increase in the number of gauche conformations of acyl chains. It was discovered that cholesterol introduces much fewer gauche conformations in the adsorbed state than in the detached state of the bilayer. In the mixed DMPC/cholesterol bilayer, a significant conformational change of the acyl chains accompanies the potential controlled phase transition from the detached to the adsorbed state of the bilayer. In contrast, in the bilayer of pure DMPC the conformational changes during the transition from the detached to the adsorbed state are negligible.

The objective of this study is to investigate the effect of cholesterol on the orientation and conformation of headgroups of DMPC molecules in DMPC/cholesterol mixed bilayers under a static electric field. The in situ photon polarization modulation infrared reflection absorption spectroscopy (PM-IRRAS) was used to monitor potential-induced changes in hydration, orientation, and conformation of DMPC headgroups in the bilayer. Combined with the results of our previous study,[7] this work provides a detailed molecular picture of the field-driven changes in orientation and conformation of DMPC molecules in a DMPC/cholesterol mixed bilayer supported at the Au (111) electrode surface.

The knowledge gained in this study may find application in basic research of a field-controlled attachment of proteins to model membrane surfaces, in the development of in vivo glucose-based bio-fuel cells and for development of biosensors.

Materials and Methods

1. Materials. 1,2-Dimyristoyl-*sn*-glycero-3-phosphocholine (DMPC, 99+%) and cholesterol (99+%) were obtained from Sigma-Aldrich (St. Louis, MO). An Au(111) single crystal was used as the working electrode (WE), a cylindrical Pt foil was used as the counter electrode (CE), and the reference was a Ag/AgCl (3 M KCl). The electrolyte for the IR experiments was 0.1 M NaF (Merck, Suprapur, Darmstadt, Germany) solution in D_2O (Cambridge Isotope Laboratories, Inc., Cambridge, MA) or H_2O (>18.2 MΩ) Milli-Q UV Plus (Millipore, Bedford, MA).

2. Methods. All the methods including vesicle solution preparation, electrochemistry, and PM-IRRAS have been described in detail previously.[7,8] To help the readers, the setup

* To whom correspondence should be addressed. E-mail: jlipkows@uoguelph.ca.

[†] Present address: Steacie Institute for Molecular Sciences, National Research Council, 100 Sussex Drive, Ottawa, Ontario, Canada K1A 0R6. E-mail: Xiaomin.Bin@nrc-cnrc.gc.ca.

10.1021/jp0660132 CCC: $33.50
Published on Web 12/07/2006

and the IR data processing procedure will be described briefly below. The PM-IRRAS setup consisted of a Nicolet Nexus 870 spectrometer, equipped with an external optical bench, MCT-A detector TRS50 MHz (Nicolet, Madison, WI), photoelastic modulator (PEM) (Hinds Instruments PM-90 with II/ZS50 ZnSe 50 kHz optical head, Hillsoboro, OR), and a demodulator (GWC Instruments Synchronous Sampling Demodulator, Madison WI). The electrode potentials were controlled via a potentiostat (EG&G, PAR Model 362, Princeton, NJ) using in-house software, an Omnic Macro, and a digital to analog converter (Omega, Stamford, CT). In addition, an Omnic Macro was used to collect and save spectra. The IR window was a BaF_2 1 in. equilateral prism. The window was washed with methanol and water and then cleaned in an ozone UV chamber (UVO-cleaner, Jelight, Irvine, CA) for 20 min prior to cell assembly.

Details concerning the PM-IRRAS spectroelectrchemical cell have been described elsewhere.[9] DMPC/cholesterol vesicles prepared in either D_2O or H_2O were injected into the electrolyte-filled cell and the solution was deaerated with argon for 2 h prior to measurement. The vesicles were allowed to fuse and spread to form a bilayer on the surface of the working electrode. The potential of the WE was set initially at -1.0 V vs Ag/AgCl and spectra were then acquired at a series of potentials, which were programmed as a cyclic sequence of 0.1 or 0.2 V potential steps. In total, 20 cycles of 400 scans each were performed to give 8000 scans at each applied potential. The resolution of the instrument was 2 cm^{-1}. At the end of the experiment, blocks of scans were individually checked for anomalies before averaging using in-house software.

The incident angle of the infrared beam and the thickness of the electrolyte layer between the prism and the electrode were adjusted individually for different spectral regions. In the C═O stretching, the maximum PEM efficiency was set to 1600 cm^{-1}. The angle of incident light was 60° and the electrolyte layer was 6.0 μm. These parameters gave comparable intensities of p- and s-polarized light inside the thin layer cavity and hence allowed for the cancellation of the IR absorption by vesicles that did not spread at the electrode surface. In the phosphate group stretching region, the PEM maximum efficiency was set to 1200 cm^{-1} ($\nu_{as}(PO_2^-)$) and 1000 cm^{-1} ($\nu_s(PO_2^-)$). The angle of incident light was 57° and the gap thickness was 6.4 and 5.0 μm for asymmetric and symmetric phosphate stretches, respectively. The thickness of the thin layer was determined by comparing the experimental reflectivity spectrum of the thin layer cell, attenuated due to the layer of solvent between the electrode and the IR window, to the reflectivity curve calculated from the optical constants of the cell constituents.[10] For C═O stretching and the symmetric phosphate stretching regions, D_2O was used as the solvent and for the asymmetric phosphate stretching the solvent was H_2O.

The demodulation technique developed in Corn's laboratory was applied in this work.[11] A modified version of a method described by Buffeteau et al.[12] was used to correct the average intensity $(I_s(\omega) + I_p(\omega))/2$ and the intensity difference $(I_s(\omega) - I_p(\omega))$ for the PEM response functions and for the difference in the optical throughputs for p- and s-polarized light. Finally, the measured spectra had to be background-corrected due to the absorption of IR photons in the thin layer cavity. The spline interpolation technique described by Zamlynny et al.[13] was used for this background correction. After these corrections, the background-corrected spectrum is a plot of $\Delta S(\omega)$, which is the absorbance of the film of adsorbed molecules,

$$\Delta S(\omega) = \frac{(I_s - I_p)}{(I_s + I_p)/2} = 2.3A = 2.3\Gamma\epsilon \qquad (1)$$

where ϵ is the decimal molar absorption coefficient and Γ is the surface concentration of the adsorbing molecules.

The method used to calculate the angle between the direction of the transition dipole of a specific vibrational mode and the surface normal has been described in detail in our previous publication.[13] This is a modified version of a method introduced by Allara and co-workers.[14,15] In brief, the integrated band intensity is proportional to the dot product between the transition dipole moment vector ($\boldsymbol{\mu}$) and the electric field vector ($\mathbf{E}$),[13−15]

$$\int A d\upsilon \propto |\boldsymbol{\mu}\cdot\mathbf{E}|^2 = \cos^2\theta |\boldsymbol{\mu}|^2 \langle \mathbf{E}^2 \rangle \qquad (2)$$

where θ represents the angle between the direction of the transition dipole and the electric field of the photon (which is normal to the surface). Using isotropic optical constants for DMPC determined by Bin et al.[8] and the optical matrix method for reflection from an interface consisting of four phases: Au/DMPC/cholesterol/D_2O/BaF_2, one may calculate the spectrum of a film of randomly oriented DMPC molecules as described in refs 8, 13, 15, and 16. The values of the thickness of the thin layer cavity and the angle of incidence used for these calculations are reported above. The thickness of the film of randomly oriented molecules was assumed to be equal to 5.5 nm, which is the thickness of the mixed DMPC/cholesterol bilayer measured by the neutron diffraction method.[17] We have performed independent neutron reflectivity[18] and AFM[19] studies of the mixed DMPC/cholesterol bilayer formed by vesicle fusion. These studies revealed that film formed at the gold electrode surface is a homogeneous bilayer that is free of unfused vesicles. With knowledge of the band intensity for a film of randomly oriented molecules, the tilt angle θ can then be calculated with the formula[13−15]

$$\cos^2\theta = \frac{1}{3}\frac{\int A_{(E)}\, d\upsilon}{\int A_{(random)}\, d\upsilon} \qquad (3)$$

where $A_{(E)}$ and $A_{(random)}$ are the absorbencies of the IR bands for the bilayer at the electrode surface and for the hypothetical bilayer consisting of randomly oriented molecules, respectively.

When eq 3 is applied to calculate the orientation of transition dipoles in the polar head region, one should take into account that hydration of the DMPC molecules at the electrode surface may be different than that in the spectrum calculated from the optical constants. Consequently, changes in the band intensity may be not only due to the change in the orientation but also hydration-induced. To estimate the effect of hydration, calculations of tilt angles were performed using optical constants determined for a solution of DMPC in CCl_4 and for a suspension of DMPC vesicles in D_2O or H_2O. When the difference between the tilt angles calculated using the two sets of the optical constants were small, the calculated tilt angles are reported. When the differences were significant, the results were rejected and in these cases the tilt angles are not reported. The error analysis for the determination of the tilt angles is described in the Appendix.

Results and Discussion

To assess the effect of cholesterol on the properties of phospholipid headgroups in the bilayer, results of DMPC/cholesterol (molar ratio 7:3) mixed bilayer studies are compared

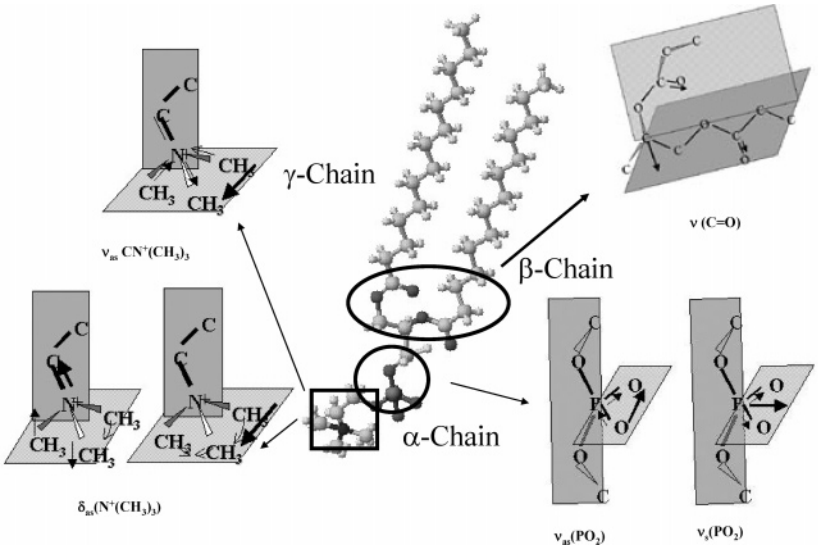

Figure 1. Schematic diagram of the DMPC molecule and the directions of the transition dipole moments of the major IR bands of the headgroup region.

to the pure DMPC bilayer described by Bin et al.[8] Figure 1 shows the molecular structure of the DMPC molecules. We are concerned here with the vibrational modes of the glycerol ester group, the symmetric and asymmetric PO_2 stretching, and asymmetric stretching and the bending modes of the choline group. Illustrations show the directions of transition dipoles of these vibrations.[8]

1. Glycerol Ester Group. Two bands of the glycerol ester group, the ν(C═O) stretch at ∼1740 cm^{-1} and the asymmetric ν_{as}(COC) stretch at ∼1180 cm^{-1} provide useful information concerning hydration of the carbonyl group and planarity of the glycerol frame. The ester carbonyl C═O stretching band is quite complex. DMPC is a mixture of two conformers, DMPC-A (80%) and DMPC-B(20%).[1b] The normal coordinate calculations by Bin et al.[7] show that the vibrations of the C═O bands in the β and γ acyl chains are coupled and as a result the bands split into two bands corresponding to the in-phase and the out-of-phase motion of atoms. In the case of the predominant DMPC-A conformation, the coupling is weak and the in-phase and the out-of-phase components are separated by 5 cm^{-1}. The transition dipoles of these bands are almost normal to the acyl chains; however, their direction rotates in the plane normal to the chains.

Figure 2a shows the C═O ester group stretching bands of pure DMPC (solid lines) and DMPC/cholesterol mixed bilayers (dashed lines). The top two spectra show the bands calculated for a 5.5 nm thick bilayer in a four-phase system: Au/DMPC/cholesterol/D_2O/BaF_2. The optical constants determined for a solution of DMPC in CCl_4 were used to calculate the top bands. The optical constants determined for a dispersion of DMPC in D_2O were used to calculate the second to the top bands. The four traces in the lower portion of the figure plot the bands of the bilayer at the Au(111) surface for selected electrode potentials. The ν(C═O) band is usually broad and composed of two overlapping bands with maxima at ∼1730 and ∼1740 cm^{-1}, which correspond to the presence of hydrogen-bonded and non-hydrogen-bonded ester groups, respectively.[19−21] In CCl_4 solution, the ν(C═O) band of pure DMPC system has a maximum at 1740 cm^{-1} and is narrower because the absorption by the non-hydrogen-bonded ester groups is predominant in this solvent. However, the ν(C═O) band of a DMPC/cholesterol mixture undergoes an obvious red shift to 1737 cm^{-1}, most likely due to a higher residual water content in this solution or eventually due to formation of a hydrogen-bonded complex with cholesterol molecule. For vesicles dispersed in D_2O, the ν(C═O) band can be de-convoluted into two bands at 1744 and 1734 cm^{-1} (pure DMPC vesicles) and at 1743 and 1730 cm^{-1} (DMPC/cholesterol mixed vesicles). In the presence of cholesterol, the band frequencies are slightly red-shifted, indicating that cholesterol facilitates hydrogen bond formation with the C═O group.

Figure 2b shows changes of the ν(C═O) band position in pure DMPC (stars and solid lines) and mixed DMPC/cholesterol (square and dashed lines) bilayers supported at the Au(111) surface, as a function of applied potential. At $E < -0.4$ V, where the bilayers are detached, the maximum of absorption of the ν(C═O) band is located at ∼1740.5 cm^{-1} (pure DMPC) and ∼1741 cm^{-1} (DMPC/cholesterol mixture), indicating that the non-hydrogen-bonded state dominates the spectrum. At $E > -0.4$ V, where the bilayer is adsorbed on the Au(111) surface, the hydrogen-bonded component grows and causes a red shift of the ν(C═O) band position. The band position of the ν(C═O) band of the DMPC/cholesterol bilayer is ∼1 cm^{-1} higher than that of the pure DMPC bilayer at the positive potential region, which may indicate that the total number of hydrogen bonds formed with carbonyl groups in DMPC/cholesterol bilayers is less than that formed in pure DMPC bilayers.

The differences between the tilt angles calculated using optical constants determined for a suspension of vesicles and a solution of DMPC in CCl_4 were less than 3°. Therefore, the changes of the ν(C═O) band reflect chiefly changes in the orientation of DMPC molecules. Figure 2c plots the mean θ of C═O for pure DMPC and DMPC/cholesterol mixed bilayer as a function of the electrode potential. As expected, the insertion of cholesterol also changes the orientation of C═O groups. At negative potentials, the tilt angle of ν(C═O) is about 70° for the pure DMPC bilayer and 67° for the DMPC/cholesterol bilayer. These angles are compared with literature results for hydrated DMPC multi-bilayer on Ge surface (64°) by Ter-Minassian-Saraga et al.[22] However, the tilt angle of ν(C═O) of DMPC/cholesterol bilayer continues to decrease as the potential changes in the positive direction and reaches 55° at the positive limit $E = 0.4$ V. The different potential dependence of the tilt angle of ν-(C═O) for pure DMPC and DMPC/cholesterol mixed bilayers indicates that the presence of cholesterol molecules in the bilayer affect somewhat the orientation of glycerol ester groups. This is in agreement with the observation that cholesterol restricts

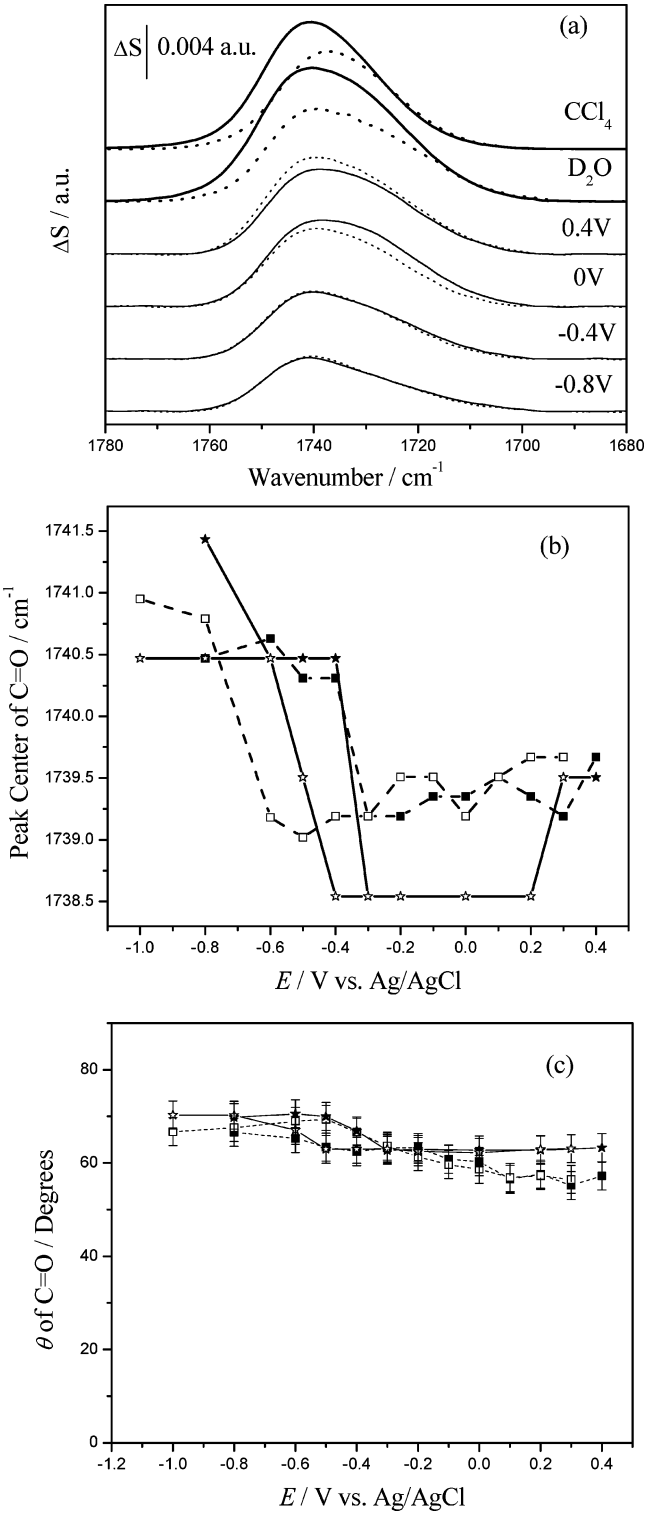

Figure 2. (a) Two top spectra marked CCl_4 and D_2O represent spectra of the bilayer calculated from the optical constants determined for the solution in CCl_4 and for the suspension of vesicles, respectively. The four bottom traces represent the PM-IRRAS spectra in the ν(C═O) stretching region, (solid line) pure DMPC bilayer, and (dashed line) DMPC/cholesterol mixed bilayer. (b) Dependence of the position of the maximum absorption frequency of the ν(C═O) stretch on the electrode potential and (c) angle between the direction of the transition dipole and surface normal; (■) positive and (□) negative potential steps for DMPC/cholesterol mixed bilayer; (closed stars) positive and (open stars) negative potential steps for pure DMPC bilayer.

freedom of motion of the carbonyl groups in DPPC multibilayers.[23] However, the differences are small and almost within the limits of experimental errors.

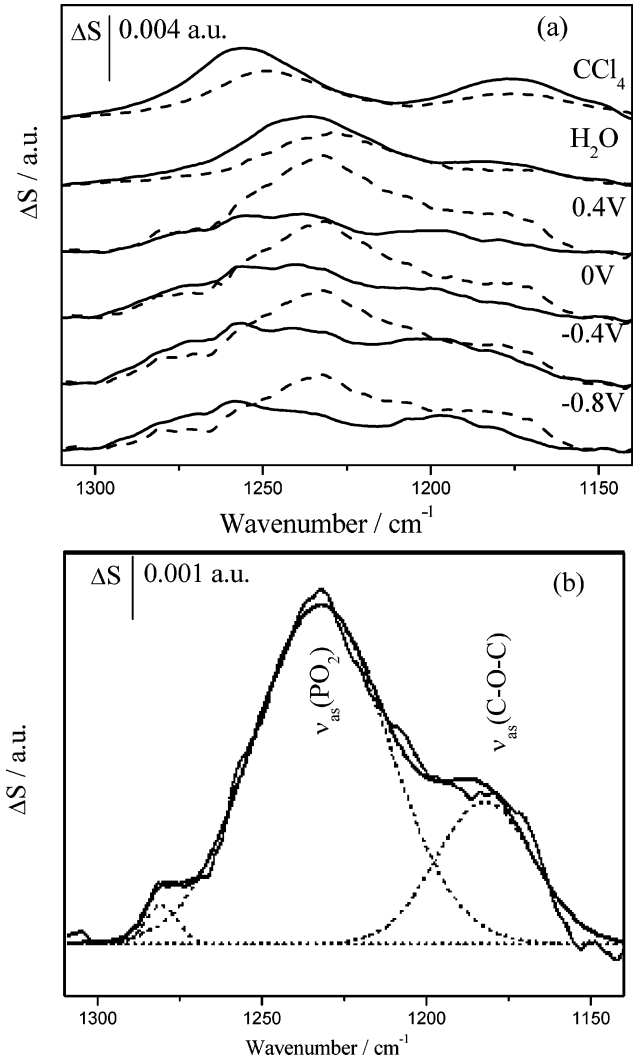

Figure 3. (a) Two top spectra marked CCl_4 and H_2O represent spectra of the bilayer calculated from the optical constants determined for the solution in CCl_4 and for the suspension of vesicles, respectively. The four bottom traces represent the PM-IRRAS spectra for the $\nu_{as}(PO^{2-})$ region, (solid lines) pure DMPC bilayer, and (dashed lines) DMPC/cholesterol mixed bilayer. (b) An example of the de-convolution of a spectrum from part (a).

The ν_{as}(COC) band is a complex band because it consists of the vibrations of the −C(O)−O−C− groups in the β and γ chains. The ester group in the γ chain is coplanar with the chain while the ester group of the β chain is out of the plane of the chain. The vibrations of the two ester −C(O)−O−C− groups are poorly coupled. However, they are strongly coupled with wagging modes of the chains.

The asymmetric C−O−C stretch of the ester groups is observed at a frequency of ∼1180 cm^{-1} and overlaps with the asymmetric PO_2^- stretch. Figure 3 shows IR bands in this spectral region. In Figure 3a, the top lines plot the band for the hypothetical bilayer of randomly oriented molecules calculated from the optical constants determined for a solution of DMPC in CCl_4 and the second top lines mark the band calculated using the optical constants determined for a solution of vesicles dispersed in H_2O. The four traces in the lower portion of the figure plot the bands of the bilayer at the Au(111) surface for selected electrode potentials. The band de-convolution is shown in Figure 3b; the shoulder peak at around 1280 cm^{-1} could be from the CH_2 wagging band progression,[23] which is not observed in the pure DMPC bilayer.

According to Fringeli,[24] the $\nu_{as}(COC)$ band is observed at 1180 cm^{-1} when the C−C(O)−O−C frame of the ester group has planar conformation. A deviation from the planar conformation leads to a red shift of this band down to ∼1160 cm^{-1}. The C−O−C band in Figure 3a is observed at ∼1184 cm^{-1} at negative potentials and ∼1181 cm^{-1} at positive potentials for the DMPC/cholesterol bilayer and ∼1190 cm^{-1} for the pure DMPC bilayer. In both cases, the peak positions are above 1180 cm^{-1}, which indicates that this band is dominated by the vibrations of the C−O−C group from the γ chain and that the C−C(O)−O−C frame has a planar conformation. Due to the large uncertainty of the background correction and a strong effect of the solvent on the intensity of this band, we do not report tilt angles for the transition dipole of this band.

2. Phosphate Group. The bands of the phosphate group include asymmetric $\nu_{as}(PO_2^-)$ and symmetric $\nu_s(PO_2^-)$ stretches of the PO_2^- moiety and bands corresponding to complex vibrations of the phosphate ester group ν(C−O[P]) and ν(P−O[C]). The asymmetric stretch of the phosphate group overlaps with the C−O−C stretch of the ester group. These bands for a pure DMPC and for a DMPC/cholesterol mixture are shown in Figure 3a. In CCl_4, the $\nu_{as}(PO_2^-)$ of the pure DMPC solution has a maximum at 1255 cm^{-1}, and the $\nu_{as}(PO_2^-)$ of DMPC/cholesterol mixture has a maximum at 1248 cm^{-1}. In an aqueous dispersion of vesicles, the band is broader and its maximum is red-shifted to 1237 cm^{-1} for pure DMPC and to 1228 cm^{-1} for the DMPC/cholesterol mixture. In the PM-IRRAS spectra, the band center of $\nu_{as}(PO_2^-)$ for the pure DMPC bilayer shifts toward lower frequencies from ∼1255 to 1246 cm^{-1} on moving from negative to positive potentials. Surprisingly, the position of the $\nu_{as}(PO_2^-)$ band center for the DMPC/cholesterol mixed bilayer does not depend on the electrode potential and is equal to ∼1232 cm^{-1}.

Figure 4a shows the 1140−1020 cm^{-1} spectral region that contains the symmetric phosphate stretch $\nu_s(PO_2^-)$ at ∼1090 cm^{-1} overlapping with ν(C−O[P]) and ν(P−O[C]) stretching bands at ∼1070 and 1055 cm^{-1}.[24−26] The deconvolution of bands in this region is shown in Figure 4b. The band assignment is taken from a recent review by Binder.[25] The C−O stretch vibration in cholesterol also has a band at ∼1050 cm^{-1}, which overlaps with the 1055 cm^{-1} ν(P−O[C]) band.[23,27] It is impossible to separate contributions of the two vibrations from the overall intensity of the ∼1050 cm^{-1} band. Overall, the uncertainty of the deconvolution of the ν(C−O[P]) and ν(P−O[C]) bands is large and we will restrict further analysis to the strong $\nu_s(PO_2^-)$ band, for which the shape and intensity depend little on the choice of the deconvolution procedure.

In the spectrum calculated from optical constants for a solution of DMPC in CCl_4, the $\nu_s(PO_2^-)$ band has a maximum at 1098 cm^{-1} for pure DMPC and 1092 cm^{-1} for the DMPC/cholesterol mixture. In the spectrum calculated from optical constants determined for a vesicle dispersion, it has a maximum at 1091 cm^{-1} for pure DMPC and 1088 cm^{-1} for the DMPC/cholesterol mixture. For the pure DMPC bilayer supported on the Au(111) electrode surface, the maximum of the $\nu_s(PO_2^-)$ band shifts from ∼1094 to ∼1089 cm^{-1} when the potential changes from −1.0 to 0.4 V. For the mixed bilayer, the $\nu_s(PO_2^-)$ band remains constant at ∼1090 cm^{-1} during the entire adsorption/desorption process, consistently with the behavior of the $\nu_{as}(PO_2^-)$ band.

The red shift of the peak position of $\nu_{as}(PO_2^-)$ and $\nu_s(PO_2^-)$ indicates an increase of hydrogen bonding associated with the phosphate groups. To compare the hydration status of the phosphate group in the pure DMPC and in the mixed DMPC/cholesterol systems, the peak positions of $\nu_{as}(PO_2^-)$ and $\nu_s(PO_2^-)$ are listed in Table 1. In CCl_4 solution, the peak positions of both $\nu_{as}(PO_2^-)$ and $\nu_s(PO_2^-)$ of the DMPC/cholesterol mixture show a red-shift compared with those of pure DMPC. In vesicle solutions, the band positions are red-shifted relative to CCl_4 solutions. The shift is quite large for the asymmetric stretch and smaller for the symmetric stretch. Further, the $\nu_{as}(PO_2^-)$ and $\nu_s(PO_2^-)$ bands appear at lower wavenumbers in mixed DMPC/cholesterol than in pure DMPC vesicles. This behavior shows that the phosphate groups are more hydrated in mixed DMPC/cholesterol than in pure DMPC vesicles. We emphasize here that the shift of the band position is observed when the state of the bilayer is changed from the detached to the adsorbed. In the adsorbed state the band position is independent of the electrode potential. On the basis of this behavior one can exclude a possibility that the shift is caused by the Stark effect.

For the pure DMPC bilayers on the Au(111) surface, positions of $\nu_{as}(PO_2^-)$ and $\nu_s(PO_2^-)$ bands exhibit a red shift when the electrode potential changes from negative to positive values.

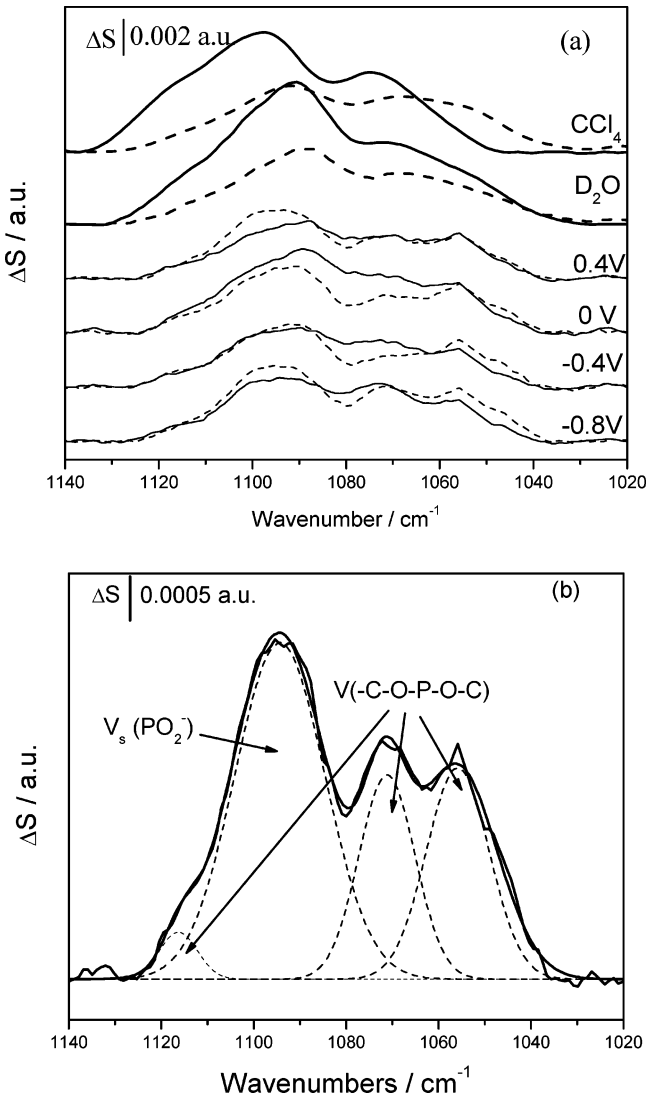

Figure 4. (a) Two top spectra marked CCl_4 and D_2O represent spectra of the bilayer calculated from the optical constants determined for the solution in CCl_4 and for the suspension of vesicles, respectively. The four bottom traces plot the PM-IRRAS spectra for the $\nu_{as}(PO^{2-})$ region, (solid lines) pure DMPC bilayer, and (dashed lines) DMPC/cholesterol mixed bilayer. (b) An example of the de-convolution of a spectrum from part (a).

TABLE 1: Positions of $\nu_{as}(PO_2)$ and $\nu_s(PO_2)$ Band Centers of Pure DMPC and DMPC/Cholesterol Mixture in CCl_4, in Solution of Vesicles in D_2O, and in Bilayers on the Au(111) Electrode Surface (cm^{-1})

	pure DMPC		DMPC/cholesterol	
	$\nu_{as}(PO_2)$	$\nu_s(PO_2)$	$\nu_{as}(PO_2)$	$\nu_s(PO_2)$
CCl_4	1255	1098	1248	1092
dispersion of vesicles	1237	1091	1228	1088
bilayers on the Au(111) electrode surface	1255 (negative *E*) to 1246 (positive *E*)	1094 (negative *E*) to 1089 (positive *E*)	1232	1090

In contrast, for the DMPC/cholesterol mixed bilayer, positions of $\nu_{as}(PO_2^-)$ and $\nu_s(PO_2^-)$ are essentially independent of potential. However, their frequencies are lower than frequencies of the phosphate bands in the pure DMPC bilayer. A recent molecular simulation study of this system by Pasenkiewicz-Gierula et al.[28] showed that the rigid structure of cholesterol and the large size of DMPC preclude a close approach of the cholesterol OH group to the DMPC headgroup in the membrane. Thus, the red shift observed here must be explained in terms of the hydrogen bonding to water. Cholesterol increases the space between the headgroups in DMPC bilayers and water molecules can penetrate more easily into the headgroup region. Similar effect of cholesterol has been reported in the literature.[29−33] The fact that positions of $\nu_{as}(PO_2^-)$ and $\nu_s(PO_2^-)$ do not depend on the potential in the mixed DMPC/cholesterol bilayer may indicate that the hydration of the phosphate group reached saturation.

Figures 3a and 4a show that the $\nu_{as}(PO_2^-)$ and $\nu_s(PO_2^-)$ peak intensities of DMPC/cholesterol bilayers are higher than those of pure DMPC bilayers. This indicates that the presence of cholesterol molecules influences the orientation of the PO_2 group significantly. Figures 5a and 5b plot angles between the surface normal and directions of transition dipoles of $\nu_{as}(PO_2^-)$ and $\nu_s(PO_2^-)$ as a function of the electrode potential, respectively. Equation 3 and optical constants determined for the aqueous suspension of vesicles were used in these calculations. In addition, we have performed the calculations using optical constants determined for a solution of DMPC in CCl_4. The differences between the two sets of data were within the reported error bars.

The transition dipoles of the asymmetric and symmetric stretches are located in the plane of the non-esterified group and are perpendicular to each other.[24,25,34] In addition, these two transition dipoles are perpendicular to the line connecting the two esterified oxygen atoms of the phosphate group. Hence, the following equation can be used to calculate the angle between the −O−P−O− line and the surface normal ($\theta\ \nu$(−O−P−O)).

$$\cos^2\theta(\nu_{as}(PO_2)) + \cos^2\theta(\nu_s(PO_2)) + \cos^2\theta(\nu(O-P-O) = 1 \quad (4)$$

The changes of this tilt angle with potential are shown in Figure 5c. For comparison Figures 5a−5c also plot the corresponding angles determined for the pure DMPC bilayer by Bin et al.[8] The data are quite scattered due to the relatively weak S/N in the spectral region of the phosphate groups. For the mixed bilayer, the angle $\theta(\nu_{as}(PO_2^-))$ changes from 46° to 36° as the electrode potential is changed from negative to positive values. The angle $\theta(\nu_s(PO_2^-))$ remains at approximately 60° at all potentials. The angle θ(−O−P−O) is ∼80° at $E < -0.4$ V and changes to ∼75° at $E > -0.4$ V. For the pure DMPC bilayer, the spectra in the 1100 cm^{-1} region reported in ref 8 were somewhat distorted due to an error in the background-correction procedure. We have repeated the analysis of this spectra and the new values of $\theta(\nu_{as}(PO_2^-))$ and $\theta(\nu_s(PO_2^-))$ are plotted in Figure 5 for comparison with data for the mixed bilayer.

The results show that, in the mixed bilayer, angles $\theta(\nu_{as}(PO_2^-))$ and $\theta(\nu_s(PO_2^-))$ are smaller and θ(−O−P−O) is higher than that for the pure DMPC bilayer. Apparently, the line connecting the two esterified oxygen atoms is less tilted with respect to the gold surface in the mixed DMPC/cholesterol bilayer. This behavior indicates that the phosphate group occupies more space in the mixed bilayer. Indeed, literature reports that presence of cholesterol increases the separation between the phospholipid groups.[29,30] With the help of a model presented in Figure 9, we will show in the summary section that these results indicate that the phosphate group is oriented with three oxygen atoms nearly parallel to the metal surface and that this orientation is essentially independent of the electrode potential.

3. Choline Group. Information concerning the choline group can be extracted from the 1500−1350 cm^{-1} region where the C−H bending modes of the methyl groups in the $N^+(CH_3)_3$ moiety are located and in the 1000−850 cm^{-1} region where C−N stretching bands are found. Figure 6a shows the spectra for the C−H bending region. For the benefit of comparison the spectra for pure DMPC are also plotted in Figure 6a. The deconvolution of these bands and the band assignment is shown in Figure 6b which shows that the asymmetric bending modes of the methyl groups ($\delta_{as}N^+(CH_3)_3$) attached to the nitrogen atom in the choline group appear at ∼1490 and ∼1480 cm^{-1} as discussed in ref 24.

Figure 7a plots spectra in the 1000−850 cm^{-1} region where the asymmetric C−N stretch ($\nu_{as}C-N^+(CH_3)_3$) at ∼970 cm^{-1} and the $-N-(CH_3)_3$ symmetric stretching modes are located. The position of the later vibrations depends strongly on the torsion angle of the −O−C−C−N− moiety. If the conformation of −O−C−C−N− is trans, the corresponding band is located at ∼930 cm^{-1}. When the conformation of −O−C−C−N− is gauche, two bands at ∼870 and ∼910 cm^{-1} are present in the spectrum.[24] Figure 7b compares spectra for the mixed and pure DMPC bilayer at $E = 0.4$ V. The spectrum of the mixed bilayer displays a band at ∼933 cm^{-1}. In contrast, this band is absent in the spectrum of the pure DMPC bilayer. This behavior indicates that the presence of cholesterol in the DMPC/cholesterol mixed bilayer changes the conformation of the −O−C−C−N− block from gauche to trans. In the spectra calculated from optical constants determined for either pure DMPC or DMPC/cholesterol mixtures in CCl_4 solution or D_2O vesicle dispersions, a broader but less pronounced peak exists in this spectral region, which may indicate that both trans and gauche conformers of −O−C−C−N− exist in CCl_4 solution or D_2O vesicle dispersions. Due to the proximity of the cutoff frequency of the BaF_2 prism (ca. 800 cm^{-1}) and the low performance of the photoelastic modulator at these low frequencies, we can only perform experiments with frequencies higher than 900 cm^{-1}.

Illustrations in Figure 8 show that the transition dipole of the $\nu_{as}(C-N^+(CH_3)_3)$ band at ∼970 cm^{-1} has the same direction as that of the ∼1480 cm^{-1} band and the $\delta_{as}(CN^+(CH_3)_3)$ mode

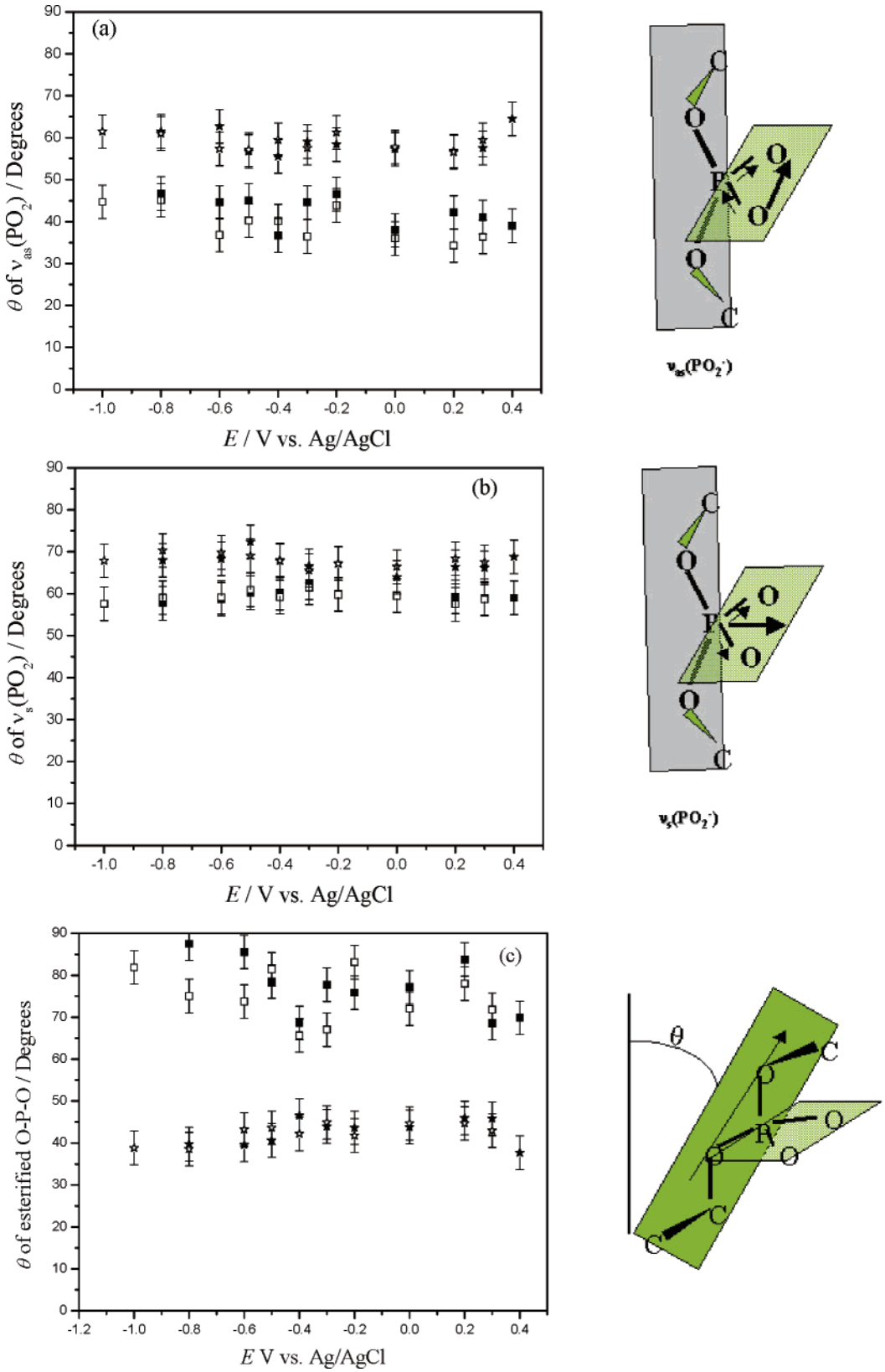

Figure 5. Dependence of the angle (θ) between directions of the transition dipole moment and the normal to the surface on the electrode potential for the DMPC/cholesterol mixed bilayer on the Au(111) electrode: (a) $\nu_{as}(PO^{2-})$ in 0.1 M NaF/H_2O solution (b) $\nu_s(PO^{2-})$ 0.1 M NaF/D_2O, and (c) tilt angle between the line connecting two esterified oxygen atoms and the surface normal; (closed symbols) positive, (open symbols) negative potential steps; (squares) DMPC/cholesterol mixed bilayer, (stars) pure DMPC bilayer.

at ~1490 cm^{-1} has its direction along the C−N bond. Figure 8 shows the potential dependence of the tilt angle of the transition dipoles of these three bands. Indeed, the angle of the ~970 cm^{-1} band $\nu_{as}(C-N^+(CH_3)_3)$ has similar magnitude as the $\delta_{as}(CN^+-(CH_3)_3)$ band at ~1480 cm^{-1}. The scatter of the data point is too large to discern any potential dependence from these data. Very similar potential independent tilt angles of ~66° were observed for the ~970 cm^{-1} and the ~1490 cm^{-1} bands in the

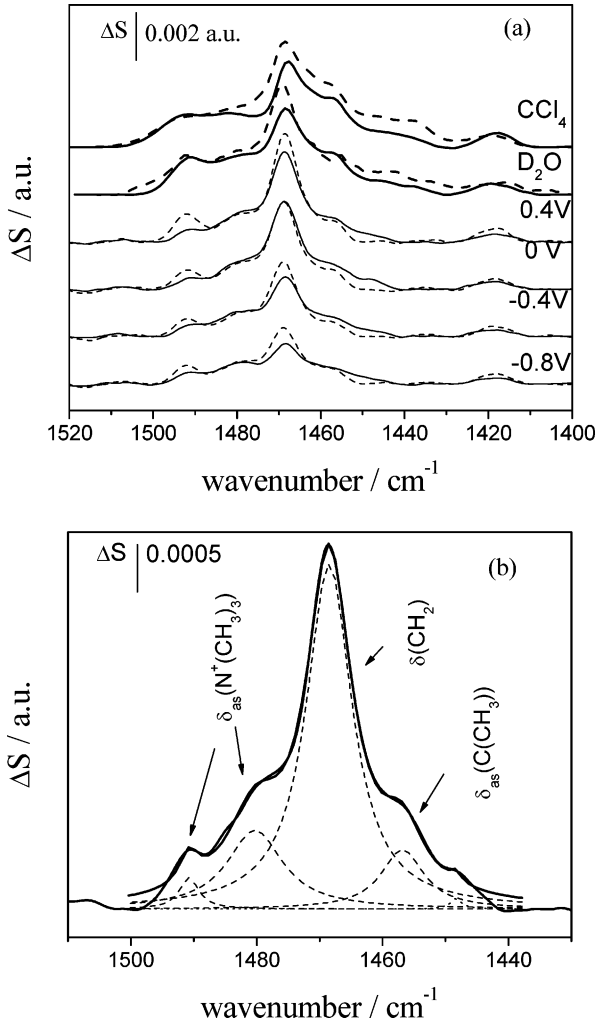

Figure 6. (a) Two top spectra marked CCl_4 and D_2O represent spectra of the bilayer calculated from the optical constants determined for the solution in CCl_4 and for the suspension of vesicles, respectively. The four bottom traces plot the PM-IRRAS spectra of the choline headgroup in the $\delta_{as}(CN^+(CH_3)_3)$ region. (b) An example of the de-convolution of a spectrum from part (a).

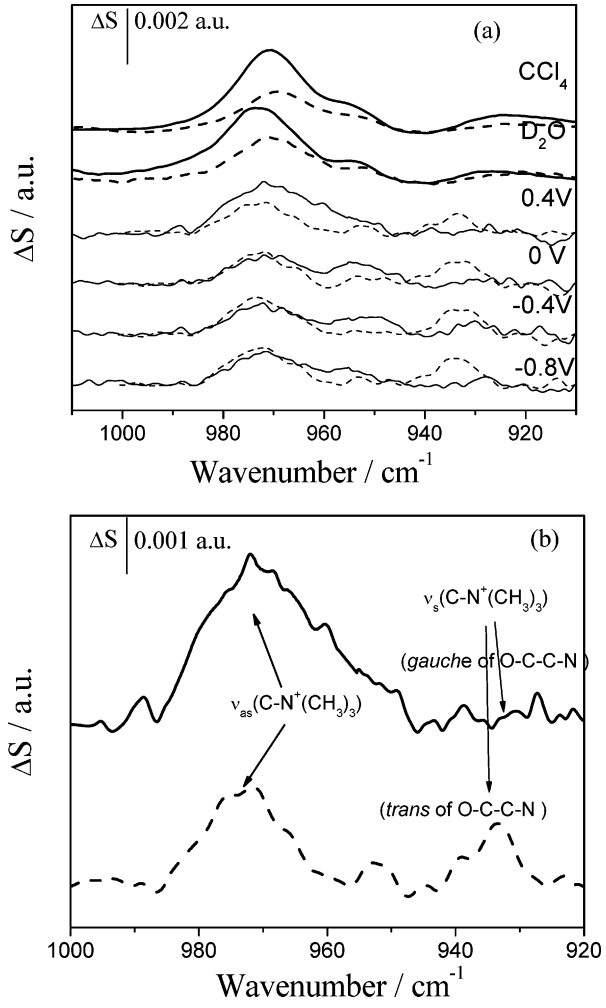

Figure 7. Two top spectra marked CCl_4 and D_2O represent spectra of the bilayer calculated from the optical constants determined for the solution in CCl_4 and for the suspension of vesicles, respectively. The four bottom traces plot the PM-IRRAS spectra of the choline headgroup in the $\nu_{as}(CN^+(CH_3)_3)$ region, (solid lines) pure DMPC bilayer; and (dashed lines) mixed DMPC/cholesterol bilayers at a Au(111) electrode in 0.1 M NaF/D_2O solution. (b) Comparison of the spectra for the supported bilayer at potential $E = 0.4$ V, (solid line) pure DMPC bilayer, and (dashed line) mixed DMPC/cholesterol bilayer.

bilayer of pure DMPC by Bin et al.[8] In this case the differences between the pure DMPC and the mixed DMPC/cholesterol bilayer are within the experimental errors. This may be a result of a free rotation of the choline group along the C−N axis.

Figure 8c shows that the angle between the C−N axis and the surface normal displays some dependence on the electrode potential. It has a value of ∼72° at $E < -0.4$ V where the bilayer is detached and it decreases to ∼64° at $E > -0.4$ V where the bilayer adsorbs on the gold surface. For pure DMPC bilayers, this angle increases from 75° to 80° when the potential changes from negative to positive values.[8] The angle changes in the opposite direction to that observed for the mixed DMPC/cholesterol bilayer. This result is consistent with a different conformation of the −O−C−C−N− moiety, trans in the DMPC/cholesterol mixed bilayer and gauche in the pure DMPC bilayer.

Summary and Conclusions

We have employed PM-IRRAS to compare properties of pure DMPC and mixed DMPC/cholesterol (molar ratio 7:3) bilayers supported at the Au(111) electrode surface, as a function the electric field applied to the electrode. The presence of 30% cholesterol was shown to influence the orientation, hydration, and conformation of DMPC molecules in the bilayer. Results of the present study and of our previous works[7,8,18] show that there are large differences between the structure of the bilayer below and above $E \sim -0.4$ V versus the Ag/AgCl reference electrode. However, these changes are more pronounced in the acyl chain section than in the polar head region of the bilayer.

At $E \sim -0.4$ V versus Ag/AgCl, the absolute value of the potential difference across the mixed bilayer is equal to ∼0.5 V.[7] This is essentially a membrane breakdown potential. The neutron reflectivity experiments by Burgess et al.[18] demonstrated that at $|E - E_{pzc}|$ higher than this breakdown potential the bilayer remains in close proximity to the electrode surface separated from the metal by a thin ∼1 nm thick cushion of the solvent. At potentials below the breakdown potential the bilayer is adsorbed, in direct contact with the metal. Therefore, we refer to the state at $E < -0.4$ V (above the breakdown potential) as to the detached state and to the state at $E > -0.4$ V potentials (below the breakdown potential) as to the adsorbed state. We discuss the differences between the structure of the adsorbed and the detached bilayers first.

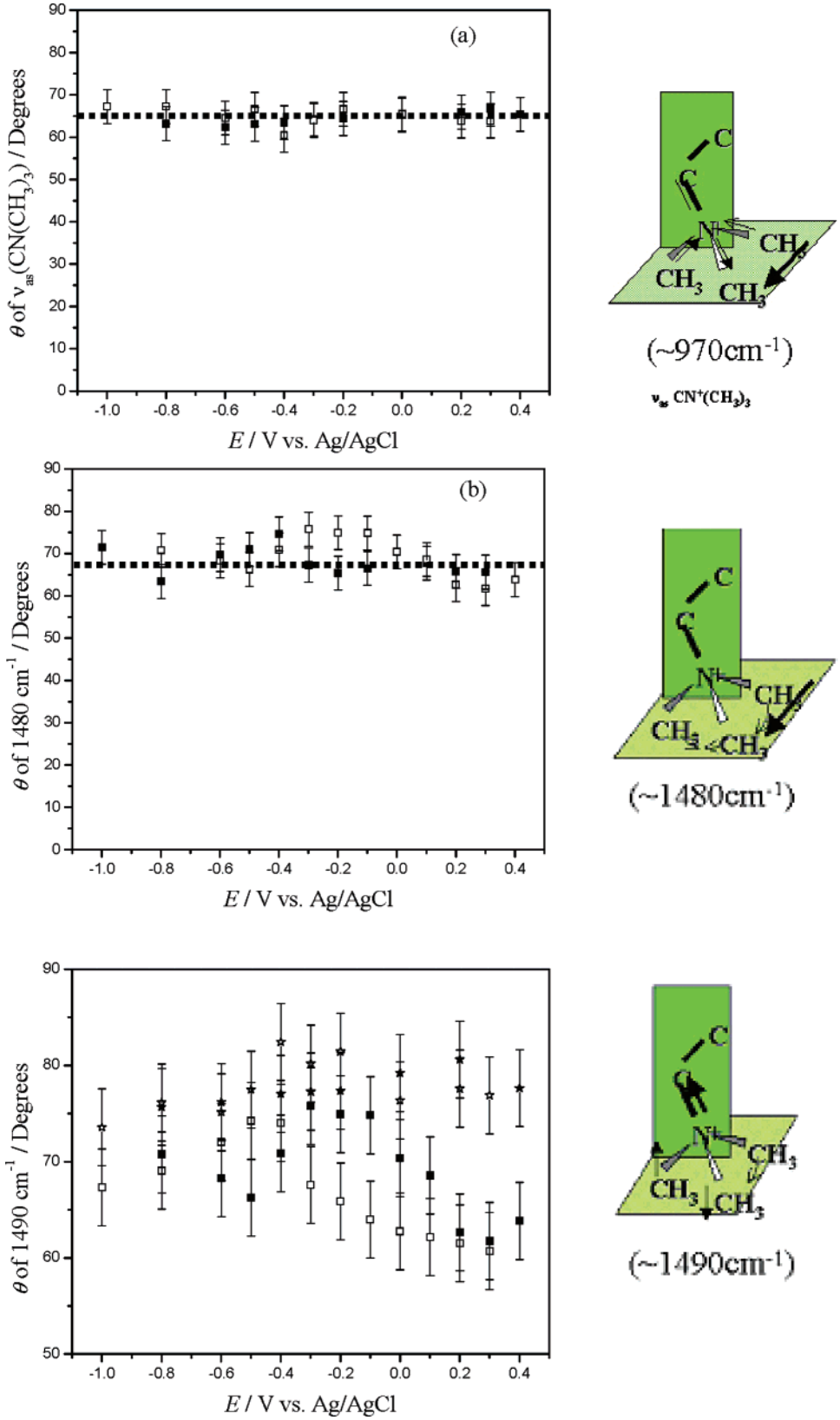

Figure 8. Dependence of the angle (θ) between the transition dipole moment and the surface normal on electrode potential for (a) $\nu_{as}(CN^{+}(CH_3)_3)$ at ~970 cm^{-1}, (b) $\delta_{as}(CN^{+}(CH_3)_3)$ at ~1480 cm^{-1}, and (c) $\delta_{as}(CN^{+}(CH_3)_3)$ at ~1490 cm^{-1}; (solid lines) pure DMPC bilayer, (dashed lines) mixed DMPC/cholesterol bilayers at the Au(111) electrode in 0.1 M NaF/D_2O; (closed symbols) positive, (open symbols) negative potential steps. The lines in panels (a) and (b) show average values.

Figure 9 combines the information concerning the orientation of acyl chains described in ref 7 with the information concerning orientation of the headgroup, determined in the present study. The molecular models show the orientation and conformation of DMPC molecules in the DMPC/cholesterol mixture (models a and b) and pure DMPC bilayer (models c and d) in two states at the gold surface: detached state at $E < -0.4$ V (models a and c) and adsorbed state at $E > 0.4$ V (models b and d). In

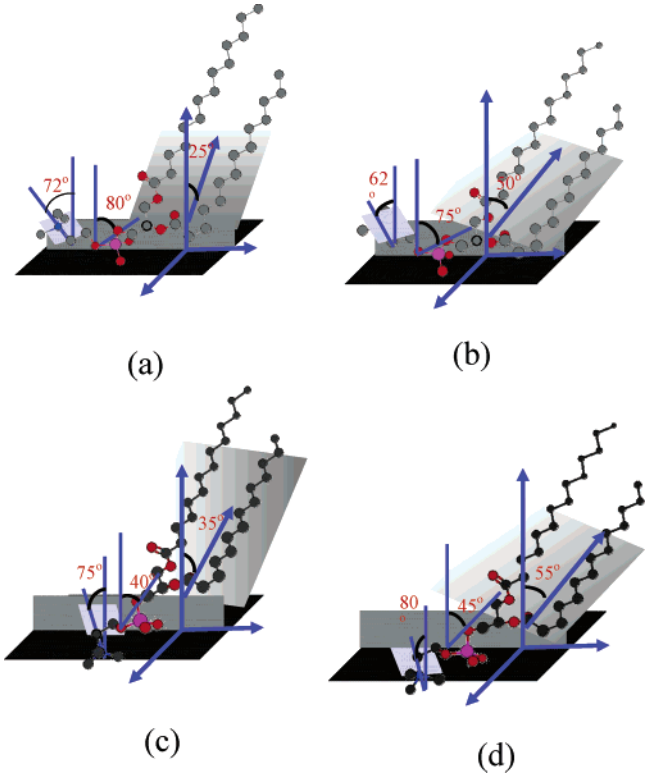

Figure 9. Orientation of the DMPC molecules in the DMPC/cholesterol bilayer at (a) $E = -0.8$ V (detached film) and (b) $E = 0.3$ V (adsorbed film) and in the pure DMPC bilayer (c) $E = -0.8$ V and (d) $E = 0.3$ V.

either the detached state or the adsorbed state of a mixed bilayer on the Au(111) surface, the tilt angle of the acyl chains with respect to the surface normal is smaller than that of acyl chains in a pure DMPC bilayer. Hence, the area per DMPC molecule decreases in the DMPC/cholesterol mixed bilayer. The addition of cholesterol also leads to an increase in the number of gauche conformations. These facts are consistent with the literature.[23,29,35] However, we have discovered an interesting new phenomenon that cholesterol introduces much fewer gauche conformations in the adsorbed state than in the detached state of the bilayer. In the mixed DMPC/cholesterol bilayer, a significant conformational change of the acyl chains accompanies the potential controlled phase transition from the detached to the adsorbed state of the bilayer. In contrast, in the bilayer of pure DMPC the conformational changes during the transition from the detached to the adsorbed state are small.

In the presence of 30% cholesterol, the conformational state of the headgroups of DMPC molecules in the mixed bilayer is also significantly changed. The phosphate group is closer to the surface compared with the pure DMPC bilayer. The conformation of the −O−C−C−N moiety changes from gauche to trans in the presence of cholesterol. The choline group rotates with potential. The presence of cholesterol also increases the hydration of the mixed bilayer.

Within the experimental error of ±4°, the orientation of DMPC molecules is essentially independent of potential in the adsorbed state of the membrane below the breakdown potential (at $E < -0.4$ V versus Ag/AgCl or $|E - E_{pzc}| < 0.5$ V). The effect of the static electric field on the structure of lipid membrane was investigated by electrochemical methods by Sargent,[36,37] Bamberg and Benz,[38] and Hianik.[39] Very precise measurements of the voltage-induced changes in the membrane capacity suggest that the polar head region of the phospholipid

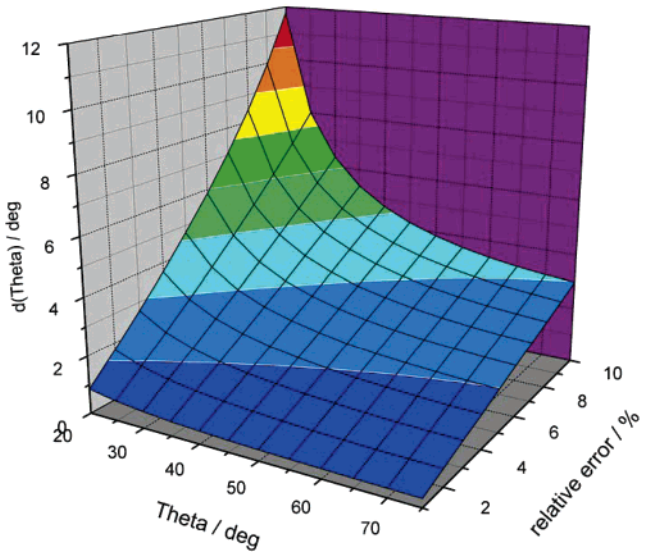

Figure 10. Plots of the error of θ (i.e., $\Delta\theta$) as a function of θ and the relative error defined as $([\Delta I_{(E)}/I_{(E)}] + [\Delta I_{(random)}/I_{(random)}])$.

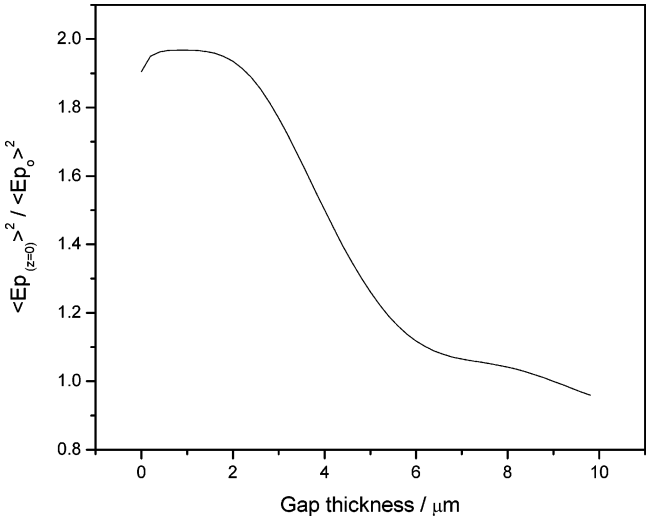

Figure 11. Enhancement of the electric field of the photon at the gold electrode surface plotted as a function of the thickness of the D_2O layer between the Au and BaF_2 window in a four-phase system consisting of BaF_2/D_2O/5.5 nm DMPC film/Au for photon frequency 1650 cm^{-1}.

molecules reorient under the influence of the electrode potential.[36,37] However, more recently Sargent[40] estimated that such changes are small, leading to the change in the orientation of the dipole by ∼1° per 100 mV of potential change across the membrane.

This estimate is consistent with ATR-FTIR spectroscopy studies of a stack of dry DMPC bilayers deposited at the surface of an ATR element by Le Saux et al.[41] and transmission experiments performed on a film of oriented multi-bilayers of DMPC formed between two Si windows Schwartzott et al.[42] Le Saux observed that a field applied to the multi-bilayer did not affect orientation of the acyl chains but caused a small change in the orientation of the polar heads. The effect was so small that no quantitative estimate of its magnitude was provided. Schwartzott et al. performed quantitative analysis of the effect of the electric field on the orientation and conformational changes in dry DMPC bilayer and concluded that electric fields on the order of 10^7 V/m have a very small effect on the orientation and conformation of the phospholipids molecule.

Our results are consistent with this literature. Within the potential range −0.4 V and 0.1 V versus Ag/AgCl, the potential difference across the bilayer supported at the gold electrode surface changes by 500 mV. We do not see any significant change in the orientation of the acyl chains or of the polar head region brought about by this change of the transmembrane voltage. However, the uncertainty of the tilt angle in our experiments is ±4°. In view of the above discussion, the precision of our measurements is not sufficient to see small field-induced changes in the orientation of the DMPC molecules.

In conclusion, we have demonstrated the power of combined spectroscopic and electrochemical studies of model membranes supported at a metal electrode surface. We also have demonstrated that a membrane that contains cholesterol is a better matrix for incorporation of peptides and proteins. The results of this work provide the background knowledge for further studies of the effect of the static electric field on the orientation and conformation of voltage-gated ion channels incorporated into a model membrane supported at the electrode surface.

Acknowledgment. This work was funded by a NSERC Discovery Grant. J.L. acknowledges the Canada Foundation of Innovation (CFI) for a Canada Research Chair Award.

Appendix: Error Analysis

The expression for the error in the determination of the angle θ (angle between the direction of the transition dipole of a given vibration and the direction of the electric field of the photon, which is normal to the surface) may be derived by differentiation of logarithms of the two sides of eq 3,

$$\Delta\theta = \frac{1}{2}\left(\left[\frac{\Delta I_{(E)}}{I_{(E)}}\right] + \left[\frac{\Delta I_{(random)}}{I_{(random)}}\right]\right)\cot\theta \qquad \text{(A-1)}$$

where $I_{(E)} = \int A_{(E)}\, d\upsilon$ is the integrated intensity of a band in the measured PM-IRRAS spectrum and $I_{(random)} = \int A_{(random)}\, d\upsilon$ is the integrated intensity of a band in the hypothetical bilayer of randomly oriented molecules calculated from the optical constants. The terms $(\Delta I_{(E)})/(I_{(E)})$ and $(\Delta I_{(random)})/(I_{(random)})$ are the relative errors of the two integrated band intensities, respectively. Figure 10 plots the error of θ (i.e., $\Delta\theta$) as a function of θ and the relative error defined as

$$\left(\left[\frac{\Delta I_{(E)}}{I_{(E)}}\right] + \left[\frac{\Delta I_{(random)}}{I_{(random)}}\right]\right)$$

The PM-IRRAS spectra were recorded using 8000 scans and hence they were recorded with a good S/N. The background correction and the band deconvolution were the main sources of errors. The band deconvolution involved a systematic error related to the choice of the function used for band fitting (Lorentzian, Gaussian, or mixed Lorentzian and Gaussian). However, the bands in the PM-IRRAS spectrum and in the spectrum calculated from the optical constants have similar shape. Therefore, the same function has always been used to deconvolute PM-IRRAS and spectra calculated from the optical constants. With use of this approach, when the same spectra were deconvoluted using different band shapes (Lorentzian or mixed Gaussian and Lorentzian), the differences between the angle θ determined from the integrated band intensities were <2°. We observed that the overall reproducibility of the integrated band intensity measurements in the PM-IRRAS spectra $[(\Delta I_{(E)})/(I_{(E)})]$ was better than 4%. One can verify the validity of this estimate by comparing the tilt angles for the transition dipoles of ∼970 and ∼1480 cm^{-1} bands of the choline group. The transition dipoles of these bands have the same direction. Indeed, very similar tilt angles were determined for these bands despite the fact that a totally different background correction and band deconvolution were involved in the calculation of these angles.

With use of the procedure described by Li et al.,[10] the optical constants can be determined with precision ∼2%. In the four-phase system, BaF_2/D_2O/DMPC/Au, the surface enhancement of the electric field of the photon at the gold electrode surface depends on the thickness of the thin layer of D_2O between Au and BaF_2. The thickness of this layer can be determined using the procedure described in ref 10 with the precision ±0.2 μm. Figure 11 shows the dependence of the enhancement of the electric field of the photon at the electrode surface as a function of the thickness of the thin layer of D_2O. When the thickness of the thin layer cavity is 6 μm, the enhancement changes slowly with the thickness. Therefore, this error contributes to the uncertainty of the intensity of the calculated spectrum <1%. Our conservative estimate of the relative error $[(\Delta I_{(random)})/(I_{(random)})]$ is ∼3%. The conservative estimate of the overall relative error

$$\left[\frac{\Delta I_{(E)}}{I_{(E)}}\right] + \left[\frac{\Delta I_{(random)}}{I_{(random)}}\right]$$

is 7%. Figure 10 shows that this uncertainty gives the error in the angle θ less than 4°.

Finally, the tilt angles reported in this work are affected by a systematic error in the estimate of the thickness of the bilayer. The value 5.5 nm used in our calculations is the upper limit. If the thickness is somewhat smaller than 5.5 nm, the tilt angles should be somewhat smaller as well. However, the same thickness of the bilayer was used to calculate θ for the pure DMPC and the mixed DMPC/cholesterol bilayer. Therefore, this error does not affect the comparison of the behavior of the bilayers with and without cholesterol and the effect of the electrode potential on the properties of these bilayers.

References and Notes

(1) (a) Dufourc, E. J.; Parish, E. J.; Chitrakorn, S.; Smith, I. C. P. *Biochemistry* **1984,** *23*, 6062. (b) Aussenac, F.; Laguerre, M.; Schmitter, J.-M.; Dufourc, E. J. *Langmuir* **2003**, *19*, 10468.

(2) Vist, R. M.; Davis, H. J. *Biochemistry* **1990**, *29*, 451−464.

(3) Presti, F. T.; Pace, R. J.; Chan, S. I. *Biochemistry* **1982**, *21*, 3831.

(4) Wong, P. T. T.; Capes, S. E.; Mantsch, H. H. *Biochim. Biophys. Acta* **1989**, *980*, 37.

(5) O'leary, T. J. In *Cholesterol in membrane models*; Finegold, L., Ed.; CRC Press: Boca Raton, FL, 1990; pp 175−196.

(6) Robinson, A. J.; Richards, W. G.; Thomas, P. J.; Hann, M. M. *Biophys. J.* **1995,** *68*, 164.

(7) Bin, X.; Horswell, S.; Lipkowski, J. *Biophys. J.* **2005**, *89*, 592.

(8) Bin, X.; Zawisza, I.; Goddard, J. D.; Lipkowski, J. *Langmuir* **2005,** *21*, 330.

(9) Zawisza, I.; Cai, X.; Zamlynny, V.; Burgess, I.; Majewski, J.; Szymanski, G.; Lipkowski, J. *Pol. J. Chem.* **2004**, *78*, 1165.

(10) Li, N.; Zamlynny, V.; Lipkowski, J.; Henglein, F.; Pettinger, B. *J. Electroanal. Chem.* **2002**, *43*, 524−525.

(11) Green, M. J.; Barner, B. J.; Corn, R. M. *Rev. Sci. Instrum.* **1991**, *62*, 1426.

(12) Buffeteau, T.; Desbat, B.; Blaudez, D.; Turlet, J. *Appl. Spectrosc.* **2000**, *54*, 1646.

(13) Zamlynny, V.; Zawisza, I.; Lipkowski, J. *Langmuir* **2003**, *19*, 132.

(14) Allara, D. L.; Swalen, J. D. *J. Phys. Chem.* **1982**, *86*, 2700.

(15) Allara, D. L.; Nuzzo, R. G. *Langmuir* **1985**, *1*, 52.

(16) Zawisza, I.; Bin, X.; Lipkowski, J. *Bioelectrochemistry* **2004**, *63*, 137.

(17) Léonard, A.; Escrive, C.; Laguerre, M.; Pebay-Peyroula, E.; Néri, W.; Pott, T.; Katsaras, J.; Dufourc, E. J. *Langmuir* **2001**, *17*, 2019.

(18) Burgess, I.; Horswell, S. L.; Szymanski, G.; Lipkowski, J.; Majewski, J.; Satija, S. *Biophys. J.* **2004**, *86*, 1763.

(19) Lewis, R. N. A. H.; McElhaney, R. N.; Pohle, W.; Mantsch, H. H. *Biophys. J.* **1994**, *67*, 2367.
(20) Blume, A.; Hübner, W.; Messner, G. *Biochemistry* **1988**, *27*, 8239.
(21) Hübner, W.; Mantsch, H. H. *Biophys. J.* **1991**, *59*, 1261.
(22) Ter-Minassian-Saraga, L.; Okamura, E.; Umemura, J.; Takenaka, T. *Biochim. Biophys. Acta* **1988**, *946*, 417.
(23) Umemura, J.; Cameron, D. G.; Mantsch, H. H. *Biochim. Biophys. Acta* **1980**, *602*, 32.
(24) (a) Fringeli, U. P. *Z. Naturforsch.* **1977**, *32b*, 20. (b) Fringeli, U. P.; Guenthard, H. H. *Mol. Biol. Biochem. Biophys.* **1981**, *31*, 270.
(25) Binder, H. *Appl. Spectrosc. Rev.* **2003**, *38*, 15.
(26) Casal, H. L.; Mantsch, H. H. *Biochim. Biophys. Acta* **1984**, *779*, 381.
(27) Paradkar, M. M.; Irudayaraj, J. *Int. J. Dairy Technol.* **2002**, *55*, 127.
(28) Pasenkiewicz-Gierula, M.; Rog, T.; Kitamura, K.; Kusumi, A. *Biophys. J.* **2000**, *78*, 1376.
(29) Yeagle, P. L. *Biochim. Biophys. Acta* **1985**, *822*, 267.
(30) Yeagle, P. L.; Hutton, W. C.; Huang, C.-H.; Martin, R. B. *Biochemistry* **1977**, *16*, 4344.
(31) Levine, Y. K. *Prog. Biophys. Mol. Biol.* **1972**, *24*, 1.
(32) McLaughlin, A. C.; Cullis, P. R.; Hemminga, M. A.; Hoult, D. I.; Radda, G. K.; Ritchie, G. A.; Seeley, P. J.; Richards, R. E. *FEBS Lett.* **1975**, *57*, 213.
(33) Jedlovszky, P.; Mezei, M. *J. Phys. Chem. B* **2003**, *107*, 5311.
(34) Zawisza, I.; Lachenwitzer, A.; Zamlynny, V.; Horswell, S. L.; Goddard, J. D.; Lipkowski, J. *Biophys. J.* **2003**, *85*, 4055.
(35) McIntosh, T. J. *Biochim. Biophys. Acta* **1978**, *513*, 43.
(36) Sargent, D. F. *J. Membr. Biol.* **1975**, *23*, 227.
(37) Sargent, D. F. Bilayer dynamics studies using capacitance relaxation. In *Molecular Aspects of Membrane Phenomena*; Kaback, H. R., Neurath, H., Radda, G. K., Schwyzer, R., Wiley, W. R., Eds.; Springer-Verlag: Berlin, 1975; pp 104−120.
(38) Bamberg, E.; Benz, R. *Biochim. Biophys. Acta* **1976**, *426*, 570.
(39) Hianik, T. *J. Biotechnol.* **2000**, *74*, 189.
(40) Sargent, D. F. *Biophys. J.* **2001**, *81*, 1823.
(41) Le Saux, A.; Ruysschaert, J. M.; Goormaghtigh, E. *Biophys. J.* **2001**, *80*, 324.
(42) Schwarzott, M.; Lasch, P.; Baurecht, D.; Naumann, D.; Fringeli, U. P. *Biophys. J.* **2004**, *86*, 285.